Validation of Vertical Refractivity Profiles as Required for Performance Prediction of Coastal Surveillance Radars

K. Naicker, F Anderson, A. le Roux
Radar and Electronic Warfare
Council for Scientific and Industrial Research (CSIR)
Pretoria, South Africa
knaicker@csir.co.za, fanderso@csir.co.za,
aleroux@csir.co.za,

S. Alhuwaimel
Electronics, Communications, Photonics (ECP)
King Abdul Aziz City for Science and Technology (KACST)
Riyadh, Saudi Arabia
alhuwaimel@kacst.edu.sa

Abstract—**Maritime border safeguarding is a vital component in the protection of a countries resources and interests against illegal activities. With the increasing asymmetric nature of today's threats, a primary requirement of any coastal surveillance system is the ability to detect small targets, such as rigid inflated boats and skiffs. The main contribution towards the radar cross section for these small targets is typically the engine and the human operator, which are approximately 1 m above the sea surface. When illuminated by a radar system, such targets are typically covered by the lowest lobes of the radar's pattern propagation factor. The behavior of these lobes is significantly influenced by the refractivity profile of the atmosphere. This paper presents the simulation of vertical refractivity profiles for modeling the detection performance of coastal surveillance radars. Validation is provided through meteorological and radio wave propagation measurements undertaken in False Bay, South Africa.**

Keywords-vertical refractive profiles, evaporation ducts, pattern propagation factor

I. INTRODUCTION

The atmosphere of the earth and the surrounding environment has a substantial effect on the propagation of electromagnetic (EM) waves. The nature of the EM wave propagation influences both the radar coverage and accuracy of the radar measurements for both earth-based radars and airborne radars used to detect earth-based targets, as discussed by Blake in [1]. The radar performance using the free space radar equation must therefore be modified to account for reflections from the earth's surface, refraction due to the inhomogeneous atmosphere and diffraction due to the curvature of the earth.

For modeling purposes, the effect of these three phenomena is included into a single quantity called the pattern propagation factor. The pattern propagation factor (PPF) is defined by Kerr in [2] as the ratio of the amplitude of the electric field at a given point under specified conditions to the amplitude of the electric field under free-space conditions with the beam of the transmitter directed towards the point in question. This paper examines the effect of refraction due to atmospheric phenomena, such as ducting, on the PFF.

The authors would like to express their gratitude to the National Program for Electronics, Communications and Photonics at the King Abdulaziz City for Science and Technology for supporting this work.

The term refraction refers to the property of a medium that causes the ray path of an EM wave to bend as it passes through that medium. In meteorology, the effect of refraction is measured using a scaled index of refraction, *M*, called the modified refractivity. For microwave frequencies, the modified refractivity in air containing water vapor can be calculated from measurements of the temperature, pressure and relative humidity of the atmosphere, and the height of these measurements above sea level as discussed in [3].

Depending on the refractivity gradient, there are four types of refractive conditions as shown in Fig. 1.

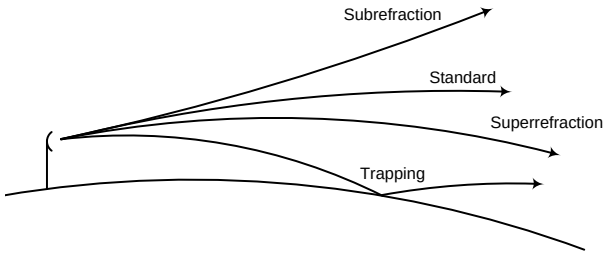

Figure 1. Types of refractive conditions

Normal refractive conditions occur when the refractivity gradient is between 79 M/km and 157 M/km and cause EM waves to bend slightly downward from a straight line. For the altitudes below 1 km the refractivity distribution can be approximated by a linear gradient. The 4/3 earth environment model assumes a linear gradient of 118 M/km, also known as the standard gradient.

When there is a temperature inversion or rapid decrease in water vapor content with height, the refractivity gradients decreases below the normal conditions. This results in the EM wave bending towards the earth more than normal. At the critical gradient (0 M/km), the EM wave will bend with a radius of curvature equal to that of the earth and travel parallel to the surface. Superrefractive gradients refer to refraction conditions between the normal and critical gradients, i.e. gradients between 0 M/km and 79 M/km.

Subrefractive conditions are anomalous conditions where the refractivity gradient is greater than 157 M/km, causing the EM wave to bend upwards.

Trapping conditions occur when the refractive gradient is less than 0 M/km. Such conditions occur for limited height extents in the troposphere. In this layer, the EM wave will bend towards the earth with a curvature smaller than that of the earth. The EM wave then encounters a layer of normal gradients and gets refracted upwards or reflects of the surface, only to re-enter the layer of the atmosphere, causing the initial downward refraction. This condition is called trapping as the EM tends to be confined in a narrow region of the troposphere.

An atmospheric duct is a horizontal layer in troposphere, where the refractive conditions are such that an EM wave will be channeled or guided as discussed above. This results in EM wave propagation over great ranges.

In a littoral environment, evaporation ducts are of particular importance, as they occur nearly permanently over the ocean. Evaporation ducts form due to the rapid decrease in the water vapor content in the layer immediately above the sea interface. The modified refractivity profile for an evaporation duct is shown in Fig. 2.

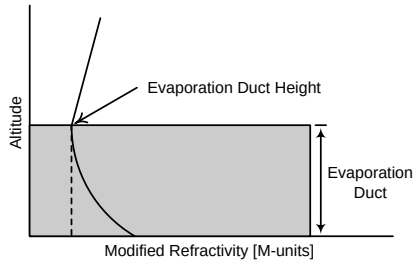

Figure 2. Evaporation duct

Fig. 3 shows the PPF for radar system deployed 110 m above sea level (ASL) for a standard atmosphere (left) and for an evaporation duct (right).

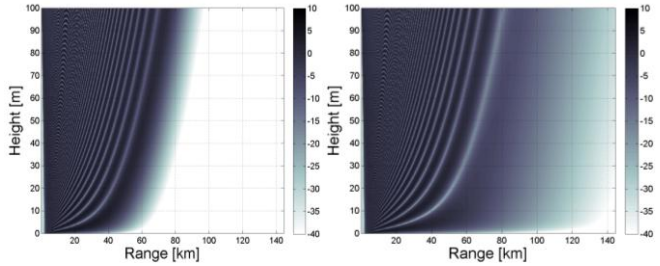

Figure 3. Pattern propagtaion factor for the standard atmosphere (left) and for the typical evaporation duct behavior for False Bay in October (right)

The effect of an evaporation duct on the behavior of the PPF is evident when comparing Fig. 3 (right) to Fig. 3 (left). For a standard atmosphere, the PFF is below -40 dB for all target heights at ranges beyond 90 km. For a 1 m target height, the PPF is less than -40 dB for ranges beyond 50 km. In contrast, when an evaporation duct is present, the PPF is in the order of -20 db for target ranges up to 120 km. An extended detection range is also possible for targets of interest, such as small boats, as the PPF is greater than -20 dB up to target ranges of 100 km.

For the scenario in Fig. 3, there is 20 dB gain in the ducting PPF when compared to the standard PPF for target ranges from 50 to 100 km. For radar applications this is equates to a 40 dB improvement, due to the two-way propagation. This is a significant improvement and equivalent to increasing the transmit power 10000 fold.

This paper presents the simulation of vertical refractivity profiles and PPF for coastal surveillance radars in False Bay and the Red Sea. The simulated ducting behavior in False Bay is validated through meteorological measurements and radio wave propagation measurements. This was a joint development, by the Radar and EW group at CSIR, South Africa and the ECP programme at King Abdul Aziz City for Science and Technology (KACST), Saudi Arabia.

II. SIMULATIONS

The Advanced Refractive Effects Prediction System (AREPS) software can be used to compute the performance of radar systems. AREPS uses the Advanced Propagation Model (APM) to compute the EM propagation under specified atmospheric refractive conditions and outputs height versus range displays of the received signal power, propagation loss, PPF and probability of detection.

For specifying the refractivity profile, AREPS contains the long term statistical frequency distribution of evaporation ducts across the world. The earth is divided in 10 degree Marsden squares. The False Bay and Western Cape coastline of South Africa is contained in Marsden 442 and the Red Sea is covered by Marsden 105.

For each Marsden square the average evaporation ducting behavior is provided for each month of the year. The vertical refractivity profiles for selected months in False Bay and the Red Sea are shown in Fig. 4 (left) and Fig. 4 (right), respectively.

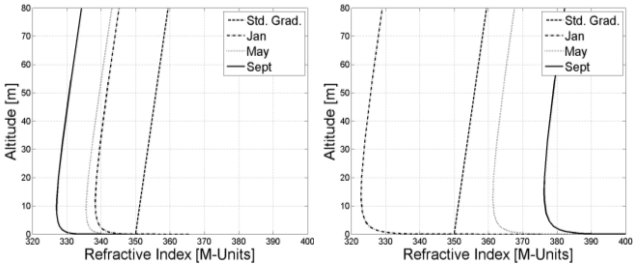

Figure 4. Vertical refractivity profiles for False Bay (left) and the Red Sea (right)

For both geographic regions, the refractivity gradient is approximately standard (118 M/km) for heights above 30 m. Below 30 m, the modified refractivity displays subtle changes in shape, depending on the evaporation duct height. The evaporation duct heights in False Bay are 11.07 m, 8.75 m and 9.07 m for January, May and September, respectively. In the Red Sea the evaporation duct height is 14.04 m, 13.31 m and 15.18 m for January, May and September, respectively.

The absolute value of the modified refractivity is proportional to both the temperature and relative humidity. Hence, the summer months have a much higher refractive index value as compared to the winter months, bearing in mind that summer in southern hemisphere corresponds to winter in the northern hemisphere.

The hot and humid climate in the Red Sea results in refractive index values much higher than that in False Bay, which has a Mediterranean climate. For each geographical location, the refractivity profiles exhibit a similar shape and only shift along the x-axis. The months with more warm and moist conditions are further on the right and the dry and cold months are on the furthest left.

The pattern propagation factor for each of the refractivity profiles shown in Fig. 4 was simulated in AREPS and is shown in Fig. 5.

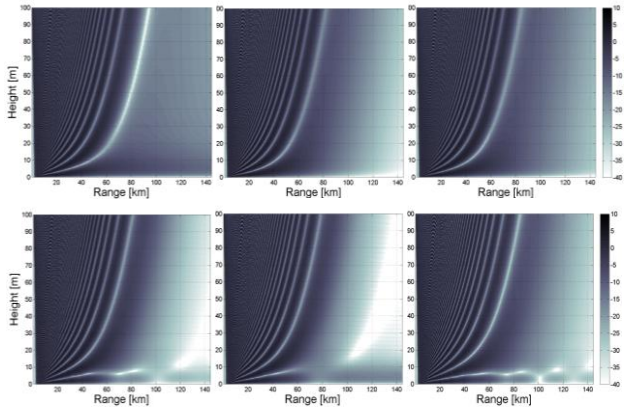

Figure 5. The pattern propagation factor for False Bay for the refractivity profiles for January (top left), May (top centre) and September (top right), and for the Red Sea for the refractivity profiles for January (bottom left), May (bottom centre) and September (bottom right),

In False Bay, it is noticed that with the increase in duct height, the energy in the lowest lobe of the PPF begins to shift to lower target heights. In January, which is the month with the highest duct height for False Bay (11.07 m), the PPF below 10 m is more than 10 dB higher than that for the other months.

In the Red Sea, it is noticed that the months with higher duct heights exhibit strong trapping conditions below 10 m. The PPF below 10 m is severely diminished at certain target ranges. In May, which is the month with the lowest duct height (13.31 m) , the power in the PPF below 10 m is considerable higher and more consistent for all ranges.

Fig. 6 shows the PPF for False Bay (left) and the Red Sea (right) for a 1 m target height. This corresponds to the case of small boat detection for a coastal surveillance radar. As shown in Fig. 6, the behavior up to 50 km is very similar for all three months and both geographical locations. At a range of 50 km, there is a 20 dB gain over the PPF for a standard atmosphere.

In False Bay for target ranges greater than 50 km, the PPF for the months with a lower duct height decrease more rapidly than the months with a higher duct height. At 100 km, there is more than a 10 dB drop in the PPF for May and September as compared to January.

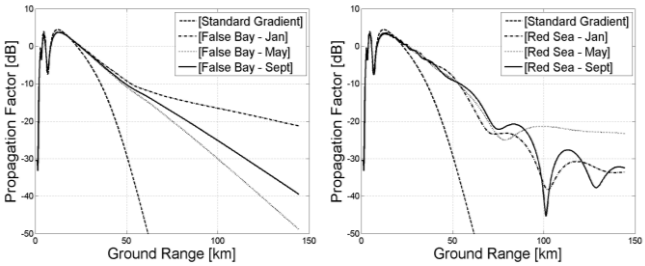

Figure 6. The pattern propagation factor for False Bay (left) and the Red Sea (right) for January, May and September for a target height of 1 m.

In the Red Sea, the PPF for May flattens to approximately 20 dB beyond 90 km. This will result in an improvement in the detection of small boats on the sea surface as compared to January and September, where the PPF displays a lobbing structure with a severe null at 100 km.

The results indicate that presence of an evaporation duct results in additional gain for ranges beyond the horizon. At 50 km there is a 20 dB additional gain for the detection of small boats for a radar height at 110 m ASL as compared to the behavior in a standard 4/3 earth environment. Knowledge of the ducting behavior is hence vital in the design of a maritime surveillance radar and should be modeled using the appropriate ducting modeling for the geographical location.

III. EXPERIMENTS IN FALSE BAY

In September/October 2010, an experimental coastal surveillance radar was deployed to Simon's Town, South Africa at an altitude of 110 m ASL. The deployment site, as shown in Fig. 7, was chosen to overlook the False Bay area.

Figure 7. Photograph of the experimental coastal surveillance radar deployed at Simons Town, overlooking False Bay.

During the deployment, several propagation measurements were undertaken. The objective was to measure the vertical refractivity profile in various locations around False Bay, over land and sea, and inspect for the presence of ducting and anomalous behavior. A propagation beacon was also placed in Gordon's bay, which is located 37 km for the deployment site on the opposite side of False Bay, with the aim of measuring the PPF across the bay. A GoogleEarth aerial photograph of the deployment site and beacon site is shown in Fig. 9.

A. Refractivity Profile Measurement Setup

A Skyhook Helikite was purchased from Allsopp Helikites and used as an aerial platform for the propagation experiments. The 11 cu m Skyhook, shown in Fig. 8 (left), is capable of

lifting a 5.5 kg payload in no wind conditions, up to an altitude of 2000 m.

The various atmospheric parameters required to calculate the refractivity profile, namely temperature, pressure and relative humidity were measured using a iMet-2-AB radiosonde purchased from InterMet Africa. The iMet-2-AB, shown in Fig. 8 (right) sampled these atmospheric parameters once every second and logged the atmospheric measurement along with the GPS time, GPS location (latitude and longitude) and altitude above the sea level.

The radiosonde was attached to the helikite, which was then repeatedly ascended and descended to perform measurements at various heights. A winch system, shown in Fig. 8 (centre), using a 12 V battery and attachable to a vehicle, was purchased to safely control the altitude of the helikite, so as to sample the altitude in 1 m steps.

Figure 8. Photograph of the11 cu m Skyhook Helikite (left), Winch setup (centre) and iMet-2-AB radiosonde (right).

Using the above mentioned setup, the vertical refractivity profile was measurements at several locations over land and sea in the False Bay area. The geographical location of these measurements relative to the radar site and beacon site is shown in Fig. 9.

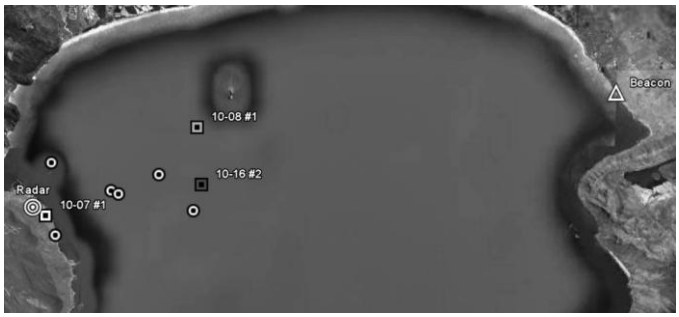

Figure 9. A GoogleEarth aerial photograph of the radar site, beacon site and locations of radiososnde measurements.

B. Measured Refractivity Profiles

On 5 October 2010, ascending and descending measurements of the refractivity profile was taken at an open area near on the Simon's Town coastline. Both measurements displayed no indication of ducting behavior, with gradients approximately that of the standard gradient.

On 7 October 2010, a single ascending measurement of the vertical refractivity profiles, shown in Fig. 10 (top), was taken to confirm the previous measurements. Again, there was no indication of ducting, demonstrating that the standard 4/3 Earth environment is suitable for modeling the refractivity conditions over land.

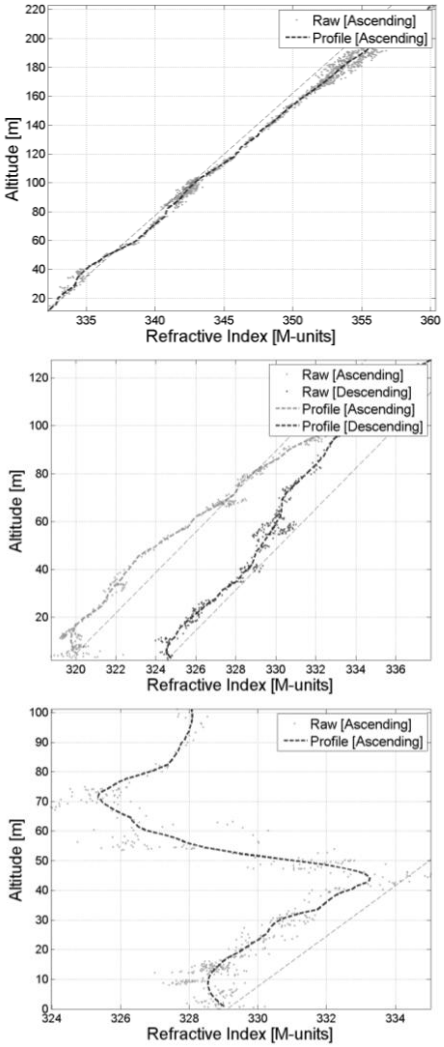

Figure 10. Vertical refractivity profile measured on 7 October 2010 (top), on 8 Oct 2010 (centre) and 16 October 2010 (bottom)

With the measurements of the refractivity profiles over land, displaying no ducting behavior, the next step was to measure the vertical refractivity profile over the sea surface. Consequently, ascending and descending measurements of the vertical refractivity profile were taken onboard a Namacurra on 8 October 2010. The results are shown in Fig. 10 (centre).

Both measurements shown in Fig. 10, indicate ducting behavior, in particular that of an evaporation duct. Again on the 12 October, the presence of an evaporation duct was confirmed through meteorological measurements.

On the 16 October, a warm and sunny day, the measurements of the refractivity, displayed an interesting anomalous behavior, as shown in Fig. 10 (bottom). Below 40 m, the refractivity profile displayed that of a typical evaporation duct. However, above 40 m, a second duct was observed. This could be a surface based duct, caused by a low temperature inversion layer.

From the measurements of the vertical refractivity profiles the following assumptions where made

- Refractivity profiles measured over land are approximately that of the standard gradient, especially when the wind is blowing into the sea.
- Refractivity profiles measured over the sea frequently displayed the presence of an evaporation duct, observed through the shape of the profile below 20 m.
- The evaporation duct seems to be a persistent occurrence over the bay and should be included in the modeling of coastal surveillance radar. Other types of duct phenomena and anomalous behavior do occur over the bay, although much less frequently.

C. Measurements of the PPF using the propogation beacon

A propagation beacon using a Hittite T2100 Signal Generator for a signal source and a wide-beam, linearly polarized horn antenna was setup in Gordon's Bay beach overlooking False Bay.

On 2 October 2010, PPF probing experiments were performed using the propagation beacon to transmit a CW signal towards the radar deployment site. The radar was then pointed toward the beacon and configured to receive the signal transmitted from the beacon.

The antenna of the propagation beacon was attached to a cherry picker and ascended in 0.5 m steps above the ground level. For each height, the received signal power from the propagation beacon was measured for vertical and horizontal polarization at selected frequencies to sample the X-band.

Fig. 11(left) shows the received power at various heights above the sea level for vertical polarization. For frequencies ranging from 8.5 GHz to 10.48 GHz, the height of the null varied between 7 m and 9 m AMSL. This null corresponds to the null between the first and second lobe in the PPF.

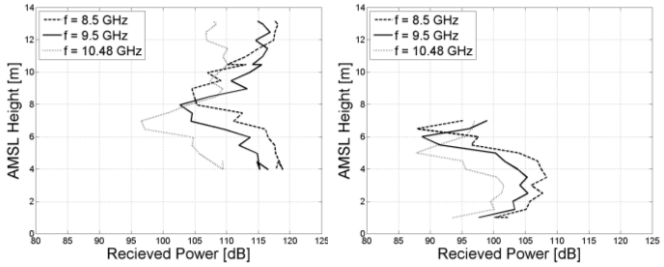

Figure 11. Received power from propagation beacon for vertical polarization

On 4 October 2010, the experiment was repeated, except this time using a long pole on the beach shore line. Fig. 11 (right) shows the received power at various heights above the sea level for vertical polarization on the beach. This time the height of the null varied between 5 m and 7 m AMSL.

Fig 12 shows the PPF for 9.5 GHz and a target range of 37 km, which is the distance between the radar and the beacon. The PPF was generated using the standard 4/3 earth's atmosphere and the ducting profiles for False Bay shown in Fig. 4 (left) For the standard gradient, one would expect the null to be approximately 13 m AMSL, denoted by the solid grey line in Fig. 12. This height is in contrast to the measured null height of 7 m and 6 m for 9.5 GHz denoted by the black line in Fig. 11 (left) and Fig. 11 (right), respectively. This would indicate that the atmospheric conditions are not that of the typical standard gradient.

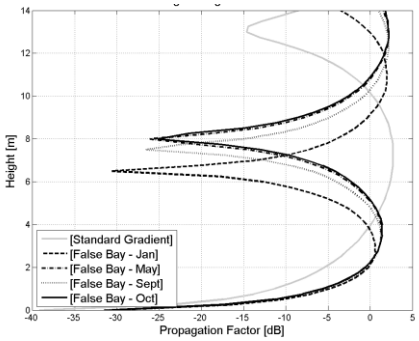

Figure 12. PPF for 9.5 GHz with a target range of 37.15 km

When an evaporation duct is taken into account, null position moves lower. In Fig. 12, the null position ranges from 6 m to 8 m over the simulated months. This behavior agrees with the measured results. These RF measurements hence confirm the presence of a stable evaporation duct.

IV. CONCLUSIONS

The meteorological measurements of the refractivity profile revealed little evidence of an evaporation duct when measured over land. When measured over the sea surface evaporation duct trends are clearly evident. RF measurements of the PPF at Gordon's Bay also indicate a lobbing structure similar to a refractivity profile with an evaporation duct as opposed the standard 4/3 Earth's refractivity profile. The expected ducting behavior was hence observed through both meteorological measurements and RF measurements.

The presence of an evaporation duct should therefore be included in the radar system design of any coastal surveillance radars. The evaporation duct models in AREPS provide a suitable means of simulating the performance of a maritime radar and have been confirmed through field trial measurements. Future work should include the evaluation of the variation of the ducting behavior for various times of the day, such as early morning, midday, evening and late nights.

ACKNOWLEDGMENT

The authors acknowledge the CSIR team involved with the measurement trial, specifically C. van Zyl, P. Barlow, R. Focke, L. Wabeke, C. Mocke , C. Venter, Y. A. Gaffar, V. Selvarajalu and L. Baben.

REFERENCES

[1] L. V. Blake, Radar Range Performance Analysis, 1st Ed., Toronto: D.C. Hearth and Company, 1980.

[2] D. E. Kerr, Propagation of Short Radio Waves, 1st Ed., New York: McGraw-Hill, 1951.

[3] User's Manual for Advanced Refractive Effects Prediction Systems, 2009